Atmospheric Environment 44 (2010) 3449–3457

Contents lists available at ScienceDirect

Atmospheric Environment

journal homepage: www.elsevier.com/locate/atmosenv

Assessment of air quality benefits from national air pollution control policies in China. Part II: Evaluation of air quality predictions and air quality benefits assessment

Litao Wang [a,b], Carey Jang [c], Yang Zhang [d], Kai Wang [d], Qiang Zhang [e], David Streets [e], Joshua Fu [f], Yu Lei [b], Jeremy Schreifels [b,g], Kebin He [b], Jiming Hao [b,*], Yun-Fat Lam [f], Jerry Lin [h], Nicholas Meskhidze [d], Scott Voorhees [c], Dale Evarts [c], Sharon Phillips [c]

[a] Department of Environmental Engineering, Hebei University of Engineering, Handan, Hebei 056038, China
[b] Department of Environmental Science and Engineering, Tsinghua University, Beijing 100084, China
[c] U.S. Environmental Protection Agency, Research Triangle Park, NC 27711, USA
[d] Department of Marine, Earth and Atmospheric Science, North Carolina State University, Raleigh, NC 27695, USA
[e] Decision and Information Sciences Division, Argonne National Laboratory, Argonne, IL 60439, USA
[f] Department of Civil and Environmental Engineering, University of Tennessee, Knoxville, TN 37996, USA
[g] U.S. Environmental Protection Agency, Washington, DC 20460, USA
[h] Department of Civil Engineering, Lamar University, Beaumont, TX 77710, USA

ARTICLE INFO

Article history:
Received 17 October 2009
Received in revised form
25 May 2010
Accepted 28 May 2010

Keywords:
Air pollution in China
Air quality modeling
Emission control
MM5/CMAQ
11th FYP

ABSTRACT

Following the meteorological evaluation in Part I, this Part II paper presents the statistical evaluation of air quality predictions by the U.S. Environmental Protection Agency (U.S. EPA)'s Community Multi-Scale Air Quality (Models-3/CMAQ) model for the four simulated months in the base year 2005. The surface predictions were evaluated using the Air Pollution Index (API) data published by the China Ministry of Environmental Protection (MEP) for 31 capital cities and daily fine particulate matter ($PM_{2.5}$, particles with aerodiameter less than or equal to 2.5 μm) observations of an individual site in Tsinghua University (THU). To overcome the shortage in surface observations, satellite data are used to assess the column predictions including tropospheric nitrogen dioxide (NO_2) column abundance and aerosol optical depth (AOD). The result shows that CMAQ gives reasonably good predictions for the air quality.

The air quality improvement that would result from the targeted sulfur dioxide (SO_2) and nitrogen oxides (NO_x) emission controls in China were assessed for the objective year 2010. The results show that the emission controls can lead to significant air quality benefits. SO_2 concentrations in highly polluted areas of East China in 2010 are estimated to be decreased by 30–60% compared to the levels in the 2010 Business-As-Usual (BAU) case. The annual $PM_{2.5}$ can also decline by 3–15 $\mu g\,m^{-3}$ (4–25%) due to the lower SO_2 and sulfate concentrations. If similar controls are implemented for NO_x emissions, NO_x concentrations are estimated to decrease by 30–60% as compared with the 2010 BAU scenario. The annual mean $PM_{2.5}$ concentrations will also decline by 2–14 $\mu g\,m^{-3}$ (3–12%). In addition, the number of ozone (O_3) non-attainment areas in the northern China is projected to be much lower, with the maximum 1-h average O_3 concentrations in the summer reduced by 8–30 ppb.

1. Introduction

As mentioned in Part I paper, the Chinese government published the 11th FYP (Five Year Plan, 2006–2010) for national environment protection in 2007. The 11th FYP set up a goal to reduce SO_2 emissions in 2010 by 10% from the 2005 level. In addition, national NO_x emission control plan is under development and might be enforced in the near future. The objective of this study is to assess the air quality benefits that would result from the planned SO_2 and NO_x emission control efforts during the 11th FYP. The Fifth-Generation NCAR/Penn State Mesoscale Model (MM5)–CMAQ modeling system is applied to simulate air quality in China.

Following the meteorological evaluations in Part I paper, this Part II presents the evaluation of air quality predictions, including

* Corresponding author. Tel.: +86 10 62782195; fax: +86 10 62773650.
E-mail address: hjm-den@tsinghua.edu.cn (J. Hao).

1352-2310/$ – see front matter © 2010 Elsevier Ltd. All rights reserved.
doi:10.1016/j.atmosenv.2010.05.058

surface concentration and column predictions for the base year 2005. The air quality changes resulting from the planned national controls are assessed.

2. Evaluation of air quality predictions

2.1. Evaluation against surface observations

Few surface air quality observation data are available to evaluate CMAQ results. The only publicly available air quality data are the daily Air Pollution Index (API) values reported by the local governments of 47 major cities in China. The API calculation and its limitations for model evaluation are briefly described below. In each of the 47 cities, an API is calculated for SO_2, NO_2, and coarse particulate matter (PM_{10}, particles with aerodiameter less than or equal to 10 μm) based on the cities average daily concentration of the pollutant. The API for the key pollutant—the maximum API value—is published as the city-wide API for that day. Using each city's API and key pollutant details, it is possible to back-calculate the daily average concentration for the key pollutant (Streets et al., 2007; Fu et al., 2009). A more detailed description can be found at the MEP's website (http://www.zhb.gov.cn/english/airqualityinfo.htm).

The use of APIs for model evaluation, however, is subject to several limitations. For example, the derived concentration of the key pollutant from API is an observed value averaged over all monitoring stations in the city. It is, therefore, not strictly comparable with the predictions of the grid cell where the city center is located. Since the exact locations of these monitoring stations are not available, it is not possible to extract model results at the same locations of these stations to calculate the corresponding predicted city-average for comparison. In addition, because only the key pollutant's API is published for the day, it may not be possible to calculate concentrations of a specific pollutant for all days if the key pollutant in the city varies.

The API data (http://www.sepa.gov.cn/quality/air.php3) for the 31 capital cities in mainland China are obtained for CMAQ model evaluation. In these cities, PM_{10} is the major air pollutant on most of the days. The simulated and API-derived PM_{10} concentrations are therefore compared. The simulated values are extracted from the grid cell where the city center is located. The monthly-mean observations are calculated when the API-derived PM_{10} concentrations are available for more than twenty days in that month.

Fig. 1 presents the spatial distribution of simulated and API-derived monthly average PM_{10} concentrations for the four months. The model generally agrees with the observed PM_{10} pollution levels in central and eastern China, especially in provinces such as Sichuan, Hubei, Hunan, Anhui, Jiangxi, Zhejiang and cities such as Shanghai and Chongqing along the Yangtze River. The four-month-average normalized mean biases for those cities are between −8% and −25%. PM_{10} concentrations are underestimated in two regions. The first is in the northwestern China, including Xinjiang, Qinghai, and Xizang provinces, where wind-blown dust is a important source of PM. The current version of CMAQ does not predict wind-blown dust so this is not included in the PM_{10} emission inventory of this study, resulting in a significant underprediction of PM_{10} for these provinces. The second region is the three provinces—Heilongjiang, Jilin, and Liaoning—in the northeastern China, where numerous heavy industries are located. The underpredictions are most likely due to uncertainties in the spatial allocation of the industrial emissions over these provinces, although the exclusion of the wind-blown dust emissions may also contribute to the underpredictions of PM_{10} in this region. In the northern China including Beijing, Tianjin, Hebei, Shanxi, and Henan, the model shows good performance in January, July, and October but underpredicts significantly in April when dust storms usually occur in this area, as a result of the exclusion of wind-blown dust emissions in CMAQ. The absence of wind-blown dust affects mostly CMAQ predictions of coarse particles with little impact on $PM_{2.5}$ predictions.

A number of statistical measures are calculated to provide a more quantitative assessment for each month, as shown in Table 1. These include the number of data pairs (n), mean observation (Mean OBS), mean prediction (Mean PRD), correlation coefficient (Corr. Coeff., R), the mean normalized bias (MNB), the mean normalized gross error (MNGE), the mean fractional bias (MFB), the mean fractional error (MFE), the normalized mean bias (NMB) and the normalized mean error (NME), for the API-derived and the CMAQ-predicted PM_{10} daily concentrations in the 31 capital cities. The formulas of these statistical measures are as follows (U.S. EPA, 2007).

$$\mathrm{MNB}=\frac{1}{n}\sum_{1}^{n}\left(\frac{(\mathrm{PRD}-\mathrm{OBS})}{\mathrm{OBS}}\right);\ \mathrm{MNGE}=\frac{1}{n}\sum_{1}^{n}\left(\frac{|\mathrm{PRD}-\mathrm{OBS}|}{\mathrm{OBS}}\right);\ \mathrm{MFB}=\frac{2}{n}\sum_{1}^{n}\left(\frac{(\mathrm{PRD}-\mathrm{OBS})}{(\mathrm{PRD}+\mathrm{OBS})}\right);$$

$$\mathrm{MFE}=\frac{2}{n}\sum_{1}^{n}\left(\frac{|\mathrm{PRD}-\mathrm{OBS}|}{(\mathrm{PRD}+\mathrm{OBS})}\right);\quad \mathrm{NMB}=\frac{\sum_{1}^{n}(\mathrm{PRD}-\mathrm{OBS})}{\sum_{1}^{n}\mathrm{OBS}};\quad \mathrm{NME}=\frac{\sum_{1}^{n}|\mathrm{PRD}-\mathrm{OBS}|}{\sum_{1}^{n}\mathrm{OBS}}. \tag{1}$$

According to the new guidance on $PM_{2.5}$ modeling published by U.S. EPA in 2007, MFB, MFE, NMB, and NME are the key statistical performance indicators (U.S. EPA, 2007). Boylan (2005) proposed an MFB less than or equal to ±60%, and an MFE less than or equal to 75%. Morris et al. (2005) proposed an MFB less than or equal to ±50% and an MFE less than or equal to 75%. If we apply this guidance on the PM_{10} evaluation in this study, the statistics in January and October meet the criteria. But the MFB and MFE of the April predictions exceed the statistical criteria. This underestimation is due primarily to the exclusion of wind-blown dust emissions in the CMAQ modeling. In the July prediction, the MFB (71%) exceeds the criteria (±50%), in part, because of the greater uncertainties in the summertime meteorological predictions.

Data from individual monitors in China are very sparse and not publicly available. Continuous daily average $PM_{2.5}$ observations from a site at Tsinghua University (THU) have been recorded by the university since July 1999 (see Fig. 1 in Part I paper, marked by the diamond point). The monitoring site is located in the western suburban area of Beijing (He et al., 2001). For this study, year 2005 daily $PM_{2.5}$ observations reported by Duan et al. (2006) are used to evaluate the temporal variations of $PM_{2.5}$ concentrations in the CMAQ predictions. Fig. 2 compares the observed and simulated daily $PM_{2.5}$ concentrations at the THU site for the four months. Note that observational data are not available in January and early April. The CMAQ predictions are consistent with the observed daily variations and seasonality during the time period when observations are available, although it tends to underpredict the magnitudes of $PM_{2.5}$ on certain days (e.g., July 22–21 and Oct. 3–8).

2.2. Evaluation against satellite observations

To overcome the shortage of the surface observations, satellite data are used to assess the column predictions including tropospheric NO_2 column abundance and AOD. Fig. 3 compares the

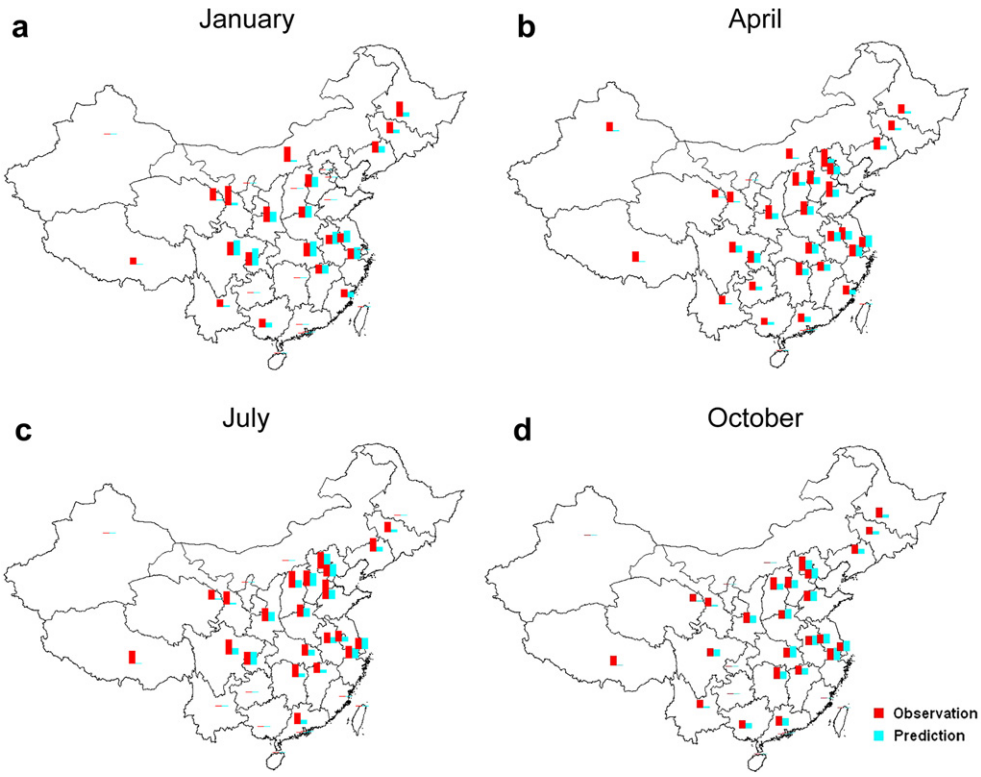

Fig. 1. Observed and predicted monthly PM_{10} concentrations in capital cities in China. The observed concentrations are derived from reported Air Pollution Index (API) by each city, and the predicted values are taken from the 2005 base case simulation.

predicted monthly-mean tropospheric NO_2 column with the observations from the Ozone Measurement Instrument (OMI) on the Aura Satellite. The OMI data are derived from its Level 2 NO_2 products with the spatial resolution of 13×24 km^2, and then processed into monthly average, as well as the CMAQ results. The model predictions agree with the observed variations, both spatially and seasonally. The observed NO_2 column mass observations are the highest in January, followed by October, April, and July; CMAQ predictions match well. Fig. 3 shows that the high NO_2 column masses over the three biggest city clusters in China—the greater Beijing area, the Yangtze River Delta, and the Pearl River Delta—are well represented by the model results and consistent with the remotely-sensing data. Observations over other polluted areas, such as larger cities in the southern Hebei Province, Taiyuan city in Shanxi Province, several industrial cities in southeastern Sichuan Province, and major cities in Korea and Japan are also reproduced by the model. In addition, the simulated spatial distributions of the NO_2 column masses along the coastlines are fairly close to the observations. Table 2(a) summarizes performance statistics of monthly-mean NO_2 column abundance. The predictions correlate well with the observations with correlation coefficients of 0.86, 0.80, 0.81, and 0.88 for January, April, July, and October, respectively. All the biases are small (less than 2%), indicating a good agreement. In the most polluted months, i.e., January and October, the model overpredicts the NO_2 column in eastern China (see Fig. 3), which may indicate larger uncertainties in the emissions during the heating season. In the Qinghai and Xizang areas, CMAQ slightly overpredicts the NO_2 column for all months except July.

Table 1
Performance statistics for API-derived daily PM_{10} concentration predictions at 31 capital cities.

Variables[a]	January	April	July	October
n	713	839	709	778
Mean OBS, μg m^{-3}	145	134	94	111
Mean PRD, μg m^{-3}	101	68	51	83
Corr. Coeff.	0.15	0.32	0.45	0.45
MNB, %	−20	−47	−46	−23
MNGE, %	50	54	52	47
MFB, %	−44	**−76**[b]	**−72**[b]	−43
MFE, %	65	**82**[b]	73	61
NMB, %	−30	−49	−45	−25
NME, %	51	55	51	46

[a] *n*—Number of data pairs. Mean OBS—mean observation. Mean PRD —mean prediction. Corr. Coeff.—correlation coefficient. MNB—the mean normalized bias; MNGE—the mean normalized gross error; MFB—the mean fractional bias; MFE—the mean fractional error; NMB—the normalized mean bias; NME—the normalized mean error.

[b] All MFB $\geq \pm 50\%$ and MFE $\geq 75\%$ are considered to indicate a relatively poor performance in this study and are highlighted in bold.

AOD can be used as an indicator of $PM_{2.5}$ pollution (Wang and Christopher, 2003; Kumara et al., 2007; Paciorek et al., 2008). In this study, observed AOD values are derived from the level 2 collection 5 aerosol products of the National Aeronautics and Space Administration (NASA)'s Moderate Resolution Imaging Spectroradiometer (MODIS) sensor aboard the Terra satellite. MODIS-derived total AODs at a wavelength of 550 nm are used to evaluate the model results. The accuracy of the MODIS AOD retrievals has been validated for some regions in China such as Beijing, Hong Kong, Taiwan, etc. (Li et al., 2003, 2005; Chen and Yang, 2005; Papayannis et al., 2006; Mi et al., 2007). Wang et al. (2007) evaluated the MODIS AOD data systematically over China using the Chinese Sun Hazemeter Network (CSHNET) and found that the correlation coefficient (R) between the MODIS data and CSHNET results was 0.72 with 44% of the data falling within the expected error issued by NASA. There were large differences in data accuracy

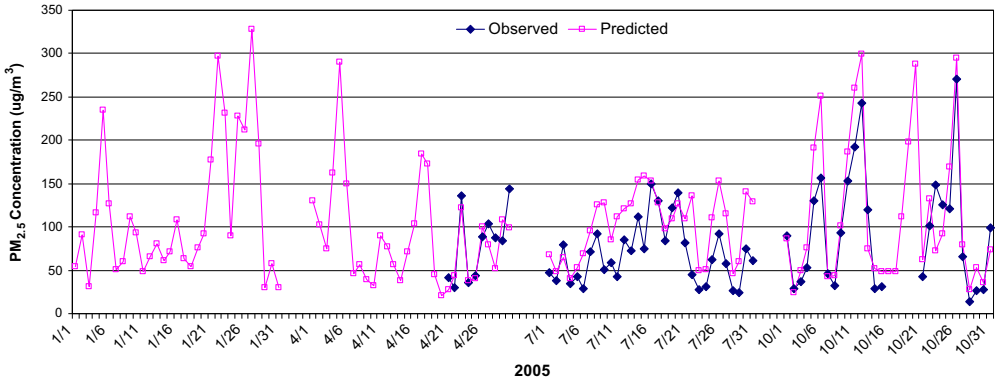

Fig. 2. Observed and predicted daily-mean $PM_{2.5}$ concentrations at the Tsinghua University (THU) site in Beijing, China. The predicted values are taken from the 2005 base case simulation.

between different ecosystems and geographic locations. The best performance appears in the agricultural areas of central-southern China. The temperate forest, coastal regions and northeast and central agricultural areas show moderate agreement. The weakest agreement appears in northern arid and semiarid regions, remote northeast agricultural areas, the Tibetan and Loess Plateau and southern forests. And Wang et al. (2007) found that "In addition, the MODIS AOD retrievals were significantly overestimated in the northern arid and semiarid regions and underestimated in remote northeast farmlands and southern forests."

CMAQ does not directly calculate AOD. The empirical equation of Chameides et al. (2002) is used to calculate AOD based on the CMAQ-predicted concentrations of $PM_{2.5}$ components including sulfate (SO_4^{2-}), nitrate (NO_3^-), black carbon (BC) and organic carbon (OC) and assumed absorption and scattering coefficients, following the methodology developed by Zhang et al. (2009). AODs are calculated using the CMAQ predictions in all model layers.

Fig. 4 compares MODIS-retrieved and CMAQ-derived monthly-mean AOD distributions. Noted that the white areas in the MODIS figures indicate that AOD data are not available. CMAQ generally reproduces the AOD distributions. Areas with high AODs over China are identified, e.g. the Sichuan basin in April, July and October; the provinces along the middle-lower Yangtze River, including Hubei, Hunan, Anhui, Jiangxi in January and April; and Beijing with Hebei and Shandong provinces in July. These regions are within the areas where MODIS retrievals show the best or moderate agreement with CSHNET observations in the study of Wang et al. (2007). In January, CMAQ AOD values are higher than MODIS AOD values in the northwest, northeast and some of the central and southern China. This may be attributed to the difficulties in measuring AODs from satellites when residual snow/ice exist on the land in the northern and central China in January, or the systematic underprediction of the MODIS AOD retrievals for southern forest areas (Wang et al., 2007). In the April predictions, CMAQ-derived AOD values are lower than MODIS AOD values over most of the domain, especially in northwest and south China. This may be partially attributed to wind-blown dust which is not accounted for in this study. In the July prediction, the CMAQ model underestimates AODs. According to Kim et al. (2007), the MODIS AOD is at its peak in China during the summer. This may be due to the "relative contribution of various processes such as stagnant synoptic meteorological patterns, secondary aerosol formation, hygroscopic growth of hydrophilic aerosols due to enhanced relative humidity, and smoke aerosols by regional biomass burning" (Kim et al., 2007). The uncertainties in summer meteorological predictions, biomass burning emission inventories, and the particle processes of the CMAQ model might contribute to the underestimation. In the October predictions, AODs are larger than MODIS-derived values, especially in the northeast, eastern and southern China. This may be partially attributed to the underpredictions of MODIS in the northeast and southern areas of China (Wang et al., 2007).

Table 2(b) summarizes the domain-wide performance statistics for AODs. The correlation coefficients between the predictions and observations are 0.70, 0.64, 0.67, and 0.72 for January, April, July and

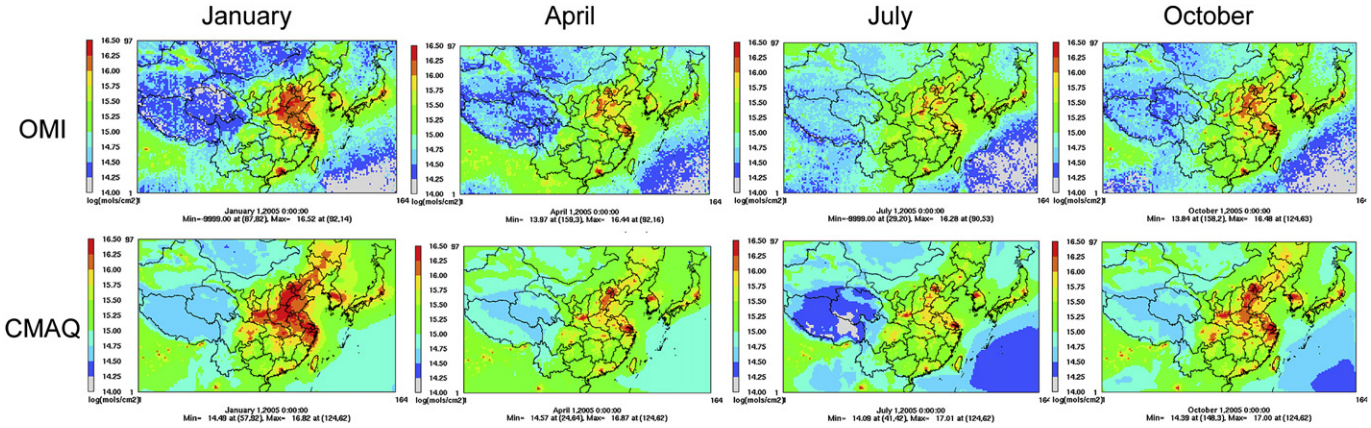

Fig. 3. Spatial distribution of monthly-mean NO_2 column abundance ($\log(\text{mol cm}^{-2})$) derived from OMI and CMAQ. The predicted values are taken from the 2005 base case simulation.

Table 2
Performance statistics for CMAQ column predictions.

Variables[a]	January	April	July	October
a. NO_2 column				
n	15,897	15,908	15,905	15,908
Mean OBS, log(mol cm^{-2})	14.89	14.96	14.93	14.92
Mean PRD, log(mol cm^{-2})	15.20	15.15	14.93	15.12
Corr. Coeff.	0.86	0.80	0.81	0.88
MNB, %	2	1	0.02	1
MNGE, %	2	2	1	2
MFB, %	2	1	0.03	1
MFE, %	2	2	1	2
NMB, %	2	1	0.03	1
NME, %	2	2	1	2
b. AOD column				
n	9895	12,389	13,589	13,636
Mean OBS	0.29	0.46	0.37	0.24
Mean PRD	0.33	0.31	0.22	0.27
Corr. Coeff.	0.70	0.64	0.67	0.72
MNB, %	40	−31	−33	53
MNGE, %	62	42	52	88
MFB, %	11	−47	−59	2
MFE, %	39	55	69	51
NMB, %	14	−34	−41	12
NME, %	42	41	48	48

[a] *n*—Number of data pairs. Mean OBS—mean observation. Mean PRD—mean prediction. Corr. Coeff.—correlation coefficient. MNB—the mean normalized bias; MNGE—the mean normalized gross error; MFB—the mean fractional bias; MFE—the mean fractional error; NMB—the normalized mean bias; NME—the normalized mean error.

October, respectively, indicating a good correlation between the CMAQ and MODIS retrieval data. The MNB, MFB and NMB in April and July are negative, showing CMAQ underestimation in these two months, as discussed above. The MFB are 0.11, −0.47, −0.59, 0.02, and MNGE are 0.39, 0.55, 0.69, 0.51 for January, April, July and October, respectively, indicating the model predictions are relatively better in January and October than in the other two months. Overall, CMAQ gives reasonably good predictions for AODs.

3. Air quality benefits of emission controls

3.1. SO_2 control benefit

The air quality benefits of emission controls can be evaluated according to the improvements in the annual concentrations of major air pollutants in China, which can be estimated by comparing the CMAQ predictions averaged over the four months under the 2010 BAU and 2010 emission control scenarios.

If the economic growth rate during the 10th FYP (2000–2005) and the existing SO_2 controls were maintained through 2010, national total SO_2 emissions in 2010 would increase by 63.7% relative to the 2005 level (2010 BAU scenario). If the 11th FYP policies for SO_2 controls are implemented successfully, the total SO_2 emissions will decline to 48% of 2010 BAU SO_2 emissions—79% of the 2005 emission level. Fig. 5 illustrates the changes to SO_2 concentrations—the difference SO_2 concentrations between the 2010 SO_2 control scenario and 2010 BAU scenario. The most polluted regions include the greater Beijing area, the Yangtze River Delta, the southern Hebei Province, Sichuan Province, and the southeastern Hubei Province. As shown in Fig. 5, these regions experience significant reductions in SO_2 concentrations under the 2010 SO_2 control scenario, particularly Beijing, Hebei, Sichuan, Hubei, and the Yangtze River Delta where the concentrations decline as much as 12–60 ppb. In most areas of the eastern China, SO_2 concentrations are reduced by 30–60%. These results clearly indicate that controlling SO_2 from power plants in China can significantly improve air quality.

Reduced SO_2 concentrations will lead to reduced SO_4^{2-} PM concentrations and total acidic deposition (sum of dry and wet deposition), because SO_2 is a precursor of SO_4^{2-} PM in the atmosphere. Figs. 6 and 7 show the decreases in the SO_4^{2-} PM concentrations and total deposition under the 2010 SO_2 control scenario. In the eastern China, the annual mean SO_4^{2-} PM concentrations declines by 2–16 $\mu g\,m^{-3}$ (12–40% decrease). The largest reduction is in the southern Hebei Province. The spatial distributions of SO_4^{2-} deposition are somewhat different from those of SO_2 or SO_4^{2-} PM concentrations, due largely to the influence of additional factors such as surface characteristics and meteorology that affect dry deposition and precipitation that affects wet deposition, and the complex interplay among those factors. Areas with high SO_4^{2-} PM deposition include Sichuan area, the southern Hebei Province, and some areas in Hubei and Anhui Provinces. The total SO_4^{2-} deposition in southern Hebei, Hubei, and Anhui Provinces are significantly reduced (by 20–50%) under the 2010 SO_2 control scenario. Since SO_4^{2-} PM is one of the major components of $PM_{2.5}$ in China (Duan et al., 2006), reduction in SO_4^{2-} concentrations lead to $PM_{2.5}$ reductions of 3–15 $\mu g\,m^{-3}$ (4–25%) in the eastern China, where the most significant reductions occur in Beijing, Hebei, Henan, and Shandong Provinces (by 8–15 $\mu g\,m^{-3}$), as shown in Fig. 8.

Visibility improvements from SO_2 controls are presented in Fig. 9. Visibility is expressed in deciview, a linear unit reflecting to perceived visual changes (Pitchford and Malm, 1994). In the 2010 BAU scenario, areas of east China, such as the southern Hebei Province, Henan, and Shandong, and the northwest China such as

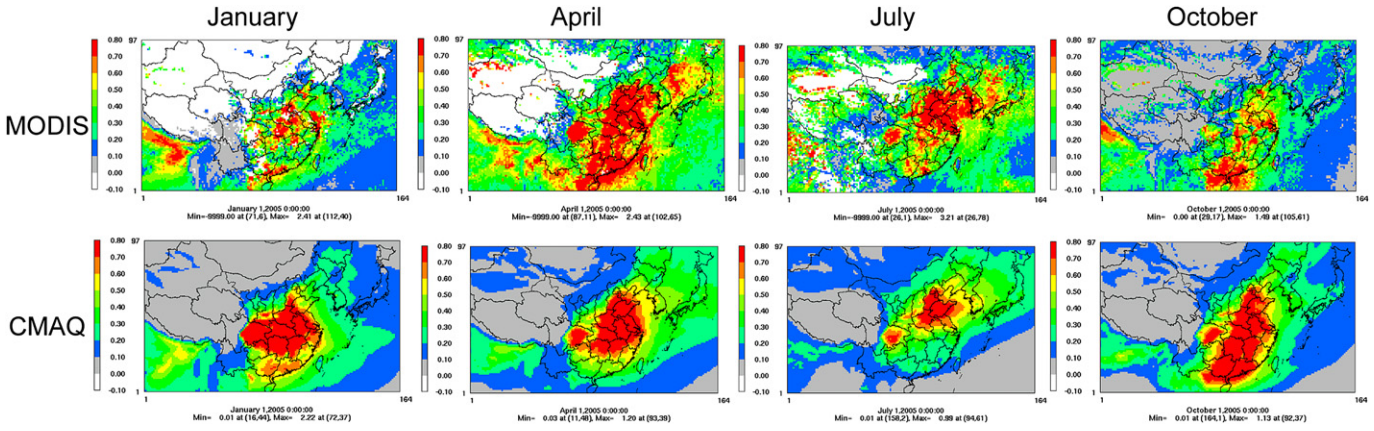

Fig. 4. Spatial distribution of monthly-mean AODs derived from MODIS and CMAQ. The predicted values are taken from the 2005 base case simulation.

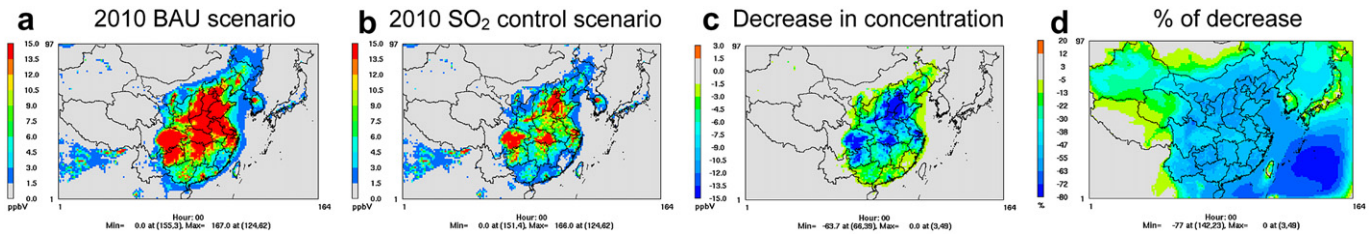

Fig. 5. Spatial distributions of annual mean SO_2 concentrations simulated by the 2010 BAU and SO_2 control scenarios ((a) and (b)), and their absolute and percentage changes due to 2010 SO_2 controls.

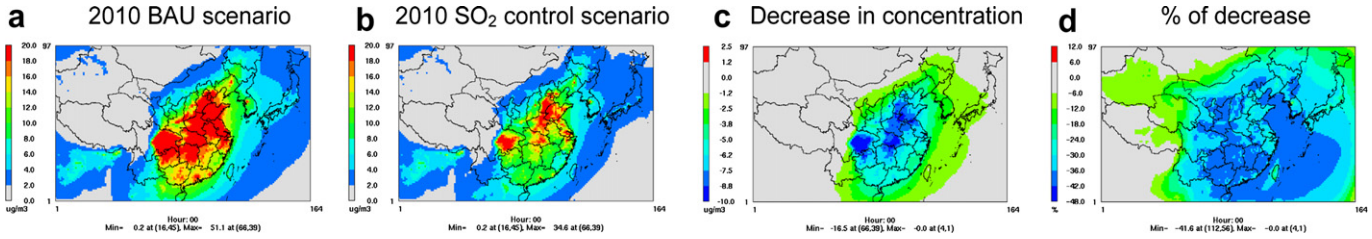

Fig. 6. Spatial distributions of annual mean SO_4^{2-} PM concentrations simulated by the 2010 BAU and SO_2 control scenarios ((a) and (b)), and their absolute and percentage changes due to 2010 SO_2 controls.

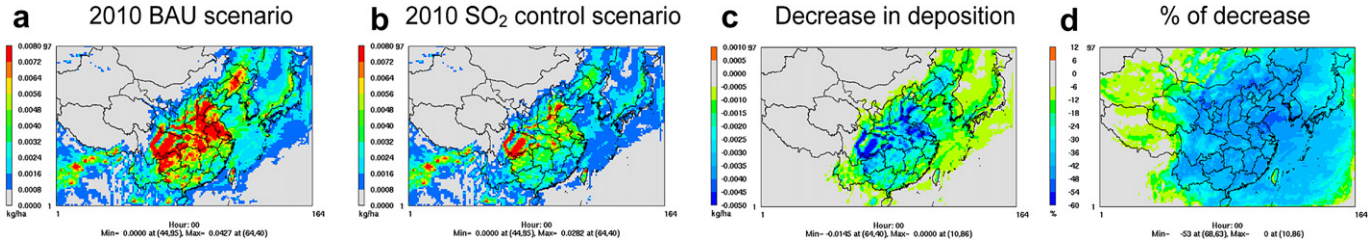

Fig. 7. Spatial distributions of annual mean SO_4^{2-} depositions simulated by the 2010 BAU and SO_2 control scenarios ((a) and (b)), and their absolute and percentage changes due to 2010 SO_2 controls.

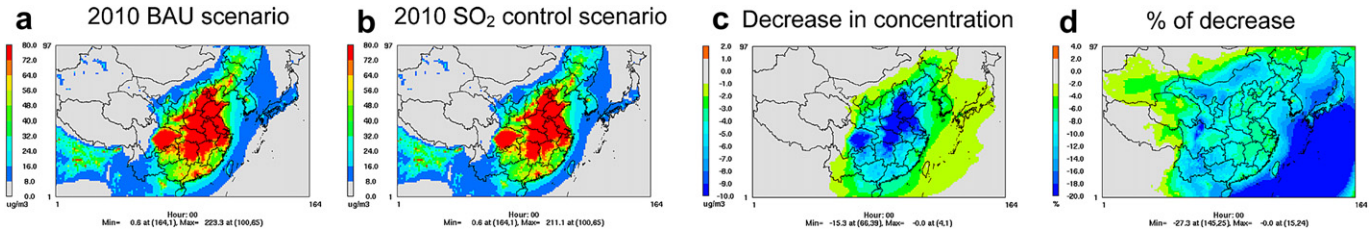

Fig. 8. Spatial distributions of annual mean $PM_{2.5}$ concentrations simulated by the 2010 BAU and SO_2 control scenarios ((a) and (b)), and their absolute and percentage changes due to 2010 SO_2 controls.

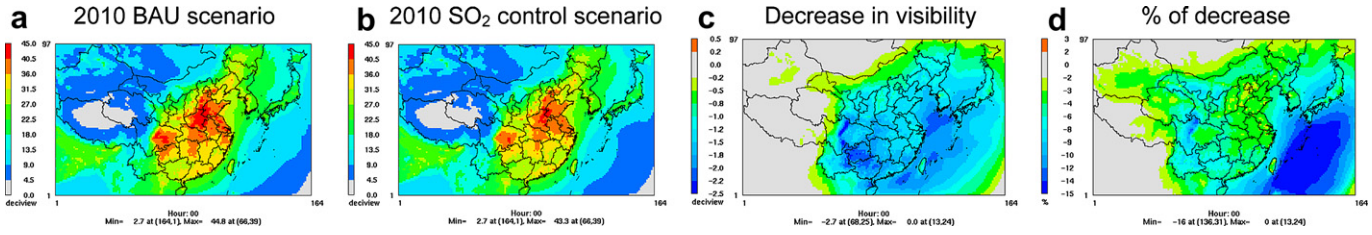

Fig. 9. Spatial distributions of annual mean visibility simulated by the 2010 BAU and SO_2 control scenarios ((a) and (b)), and their absolute and percentage changes due to 2010 SO_2 controls.

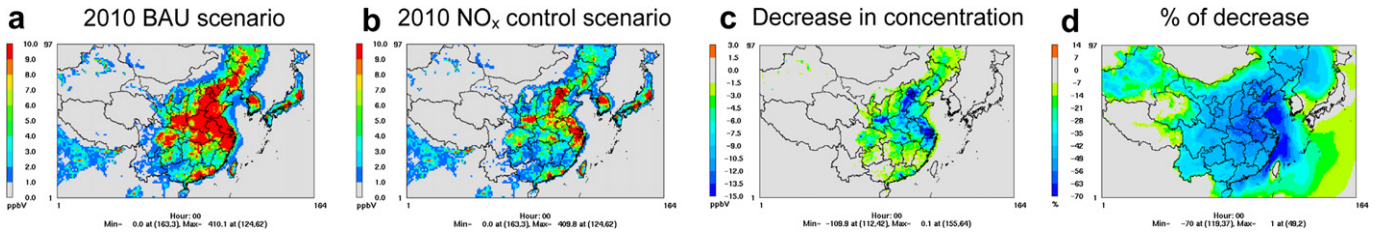

Fig. 10. Spatial distributions of annual mean NO_x concentrations simulated by the 2010 BAU and NO_x control scenarios ((a) and (b)), and their absolute and percentage changes due to 2010 NO_x controls.

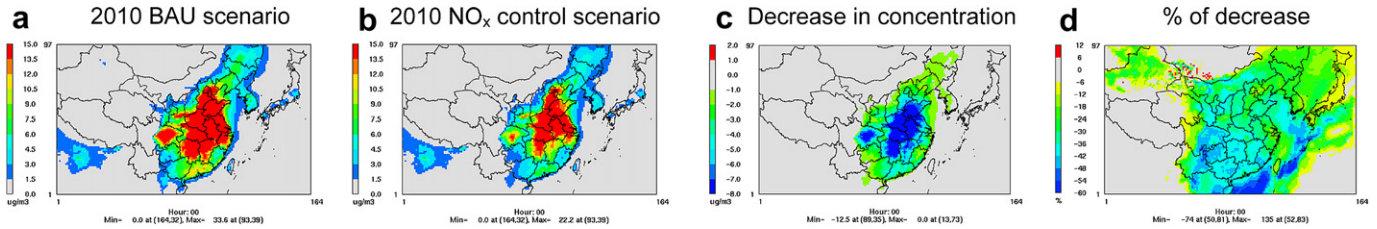

Fig. 11. Spatial distributions of annual mean NO_3^- PM concentrations simulated by the 2010 BAU and NO_x control scenarios ((a) and (b)), and their absolute and percentage changes due to 2010 NO_x controls.

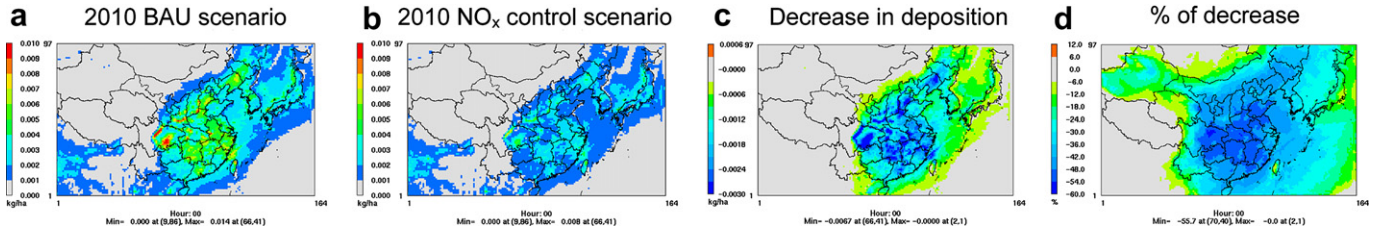

Fig. 12. Spatial distributions of annual mean NO_3^- depositions simulated by the 2010 BAU and NO_x control scenarios ((a) and (b)), and their absolute and percentage changes due to 2010 NO_x controls.

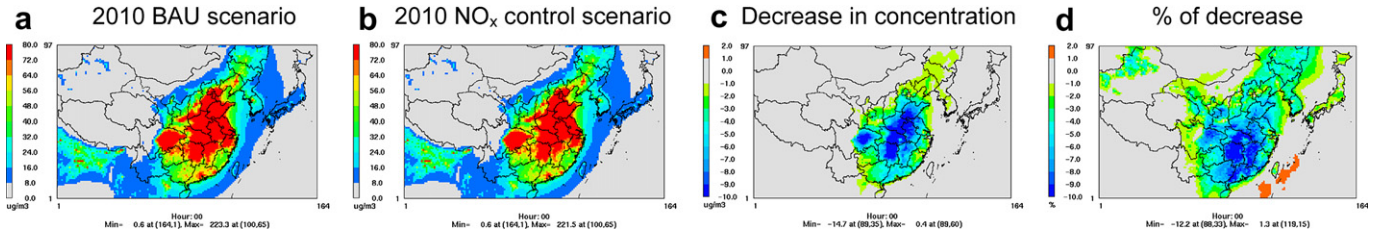

Fig. 13. Spatial distributions of annual mean $PM_{2.5}$ concentrations simulated by the 2010 BAU and NO_x control scenarios ((a) and (b)), and their absolute and percentage changes due to 2010 NO_x controls.

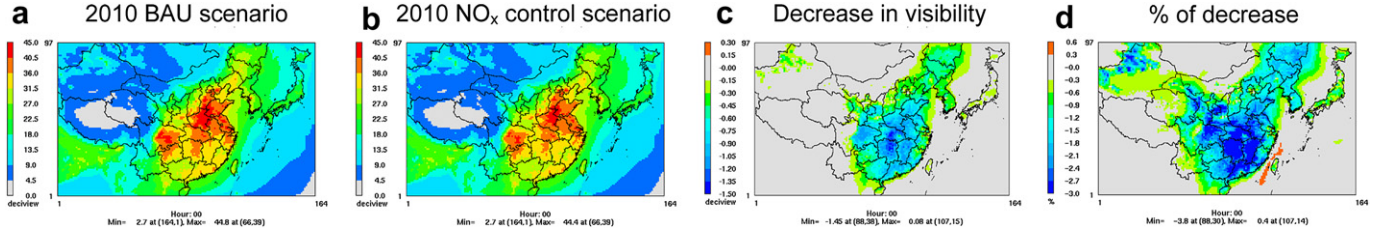

Fig. 14. Spatial distributions of annual mean visibility simulated by the 2010 BAU and NO_x control scenarios ((a) and (b)), and their absolute and percentage changes due to 2010 NO_x controls.

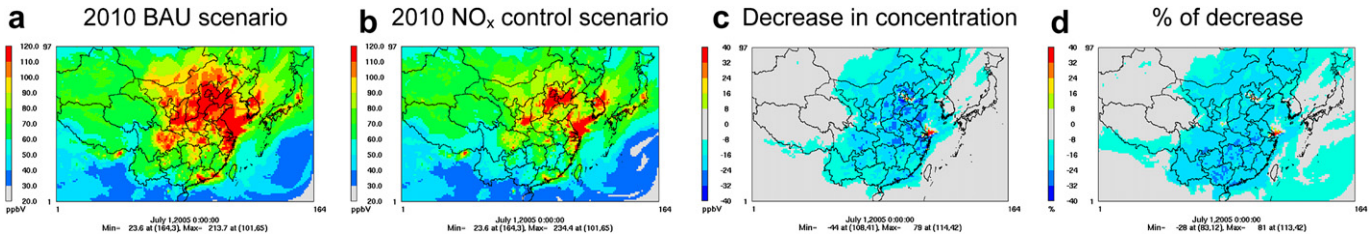

Fig. 15. Spatial distributions of maximum 1-h O_3 concentrations in July simulated by the 2010 BAU and NO_x control scenarios ((a) and (b)), and their absolute and percentage changes due to 2010 NO_x controls.

the eastern Sichuan Province, have poor visibility. The visibility in these areas is over 35 deciview, which means the visual range is less than about 12 km. Under the 2010 SO_2 control scenario, visibility improves (0.5–2.7 deciview) over most areas in China, except the three provinces of Qinghai, Xizang and Xinjiang, where visibility is good in both the 2010 BAU and SO_2 control scenarios. The largest improvement appears in the southwest China, including Guizhou and Sichuan Provinces, and the southeastern coastal area. The percentage decrease shows a similar pattern over the land. The largest percentage change appears over the southwest China including Sichuan, Yunan and Guizhou, and inner Mongolia by about 4–12% (Fig. 9(d)).

3.2. NO_x control benefit

Under the 2010 BAU scenario, the national NO_x emissions are projected to increase by 59% from the 2005 level. If NO_x controls were applied, the 2010 NO_x control scenario predicts NO_x emissions reductions of 43% below the 2010 BAU scenario – a 10% from the 2005 level.

Fig. 10 shows the change in NO_x concentrations under the 2010 NO_x control scenario relative to the 2010 BAU scenario. Heavy NO_x pollution in the eastern China under the 2010 BAU scenario can be greatly reduced (by 30–60%) under the 2010 NO_x control scenario. The greatest reductions are over the greater Beijing area, the southern Hebei Province, and the Yangtze River Delta. In these areas, annual mean NO_x concentrations decline more than 10 ppb.

Fig. 11 shows the air quality benefits in terms of reduction in NO_3^- PM concentrations. The NO_3^- PM concentrations in the eastern China decline by 2–7 $\mu g\,m^{-3}$ (20–40%). It is interesting that large reductions of NO_3^- concentrations occur in the south of the regions where maximum NO_x reduction occurs. The maximum reduction ($>6\ \mu g\,m^{-3}$) occurs in Shandong, Henan, Anhui, Hubei, and Hunan Provinces, and the eastern Sichuan Province. As for the total NO_3^- deposition (see Fig. 12), the percent reduction is 24–55% in the polluted areas of eastern China. The best improvement occurs in the eastern Sichuan Province and southern Hebei, and the Yangtze River drainage area. NO_3^- is also one of the major components of $PM_{2.5}$ (Duan et al., 2006). Fig. 13 shows 3–12% of reduction in the $PM_{2.5}$ concentrations due to NO_x control, with the largest improvement of 2–14 $\mu g\,m^{-3}$ in highly polluted areas in eastern China.

The visibility benefit of NO_x emission control is shown in Fig. 14. The improvement from NO_x controls is not as great as the improvement from SO_2 controls. The largest visibility improvement (0.9–1.5 deciview reduction) occurs in south-central China, including Hubei and Hunan Provinces. The largest percent reduction (>2.4%) also occurs in that area.

Since NO_x is one of the two major O_3 precursors, NO_x control affects O_3 pollution, particularly in summer when O_3 pollution is the most severe. Fig. 15 shows the spatial distribution of the maximum 1-h concentrations of O_3 in July under the 2010 BAU and the 2010 NO_x control scenarios. The China National Ambient Air Quality Standards (CNAAQS) for maximum 1-h O_3 concentration is 200 $\mu g\,m^{-3}$ (equivalent to approximately 100 ppb, denoted in red color in Fig. 15). Under the 2010 BAU scenario, many areas in the northern China fail to O_3 attain the CNAAQS, including the greater Beijing area, Hebei, Shandong and Shanxi Provinces, and the Yangtze River Delta. With NO_x controls, the O_3 non-attainment areas are reduced significantly to the areas of Beijing, Hebei Province and the Yangtze River Delta. Maximum O_3 concentrations decline 8–30 ppb (8–32%) in the polluted areas of northern China. It should be noted that there are some red spots in the areas of Beijing, Tianjin and Shanghai city, indicating an O_3 disbenefit (by 24–79 ppb) from NO_x control. This is consistent with the conclusions of other studies (Geng et al., 2008; Wang et al., 2008; Xu et al., 2008) that these cities are VOC-limited so that the reductions in NO_x emissions can result in higher O_3 concentrations.

4. Conclusions

In this Part II paper, the CMAQ performance is statistically evaluated for the base year 2005. The surface air quality predictions of CMAQ are evaluated by comparing with the MEP published API of 31 cities in China and the daily $PM_{2.5}$ observations at the Tsinghua University site. The model predictions are consistent with the observations. To overcome the shortage of surface observations, satellite data of the NO_2 columns from OMI and AOD from MODIS are also used to evaluate the model. The simulations show a good agreement with the OMI-derived NO_2 column masses, but relatively poor agreement with the MODIS-derived AODs. The discrepancies in AODs may be attributed to uncertainties in the CMAQ predictions resulting from the uncertainties in the particulate emission inventory, the meteorological predictions, and the physical and chemical processes in the CMAQ model, as well as the uncertainties in the MODIS-derived AODs over China, especially over the winter time.

The SO_2 emission controls planned in the 11th FYP will result in large air quality benefits across multiple air pollution problems including pollution of SO_2 and PM, and acid deposition. Relative to the 2010 BAU scenario, the annual mean SO_2 concentrations in 2010 will decline by as much as 30–60% in polluted areas of the eastern China. The annual mean SO_4^{2-} PM and $PM_{2.5}$ concentrations will decline by 2–16 $\mu g\,m^{-3}$ (12–40%) and 3–15 $\mu g\,m^{-3}$ (4–25%), respectively. The total SO_4^{2-} deposition will decline by 20–50%.

If NO_x emissions were reduced by 10%, China would experience appreciable air quality benefits, including reductions in NO_x, O_3, and PM concentrations, acid deposition, and nitrogen deposition. Relative to the 2010 BAU scenario, the NO_x concentrations under the 2010 NO_x control scenario decline by 30–60% from predictions under the 2010 BAU scenario. The NO_3^- PM concentrations and depositions decline by 20–40% and 24–55%, respectively, in the polluted areas of the eastern China. The annual mean $PM_{2.5}$ concentrations decline by 2–14 $\mu g\,m^{-3}$ (3–12%). The O_3 non-

attainment areas are greatly reduced, with the declines in maximum 1-h O_3 concentrations in July of 8–30 ppb.

The results of this study give very important implications for the development and refinement of air quality control strategies in China. To achieve the SO_2 control targets, the China MEP is accelerating the implementation of an integrated SO_2 emission monitoring system and an emission trading system. As a result, significant reduction in SO_2 and sulfate pollution is expected across China in the year 2010. Similar NO_x controls, while not already in place, are expected in the near future. If such SO_2 and NO_x control strategies are implemented successfully in China, they will result in significant multiple air quality benefits, as demonstrated in this study.

This study has several limitations. First, the same MM5 fields are used in all scenarios—future climate change and its impact on air quality are not included, which may be important. Second, both the 2010 SO_2 and NO_2 control scenarios are evaluated based on the assumption that there are no additional controls for other pollutants, which is unlikely given that China is placing significant resources and political support to reducing air pollution. The interplay of the various pollutants may result in considerable differences in air quality. Third, air quality observations are limited and there are insufficient data to evaluate the SO_2 predictions, the uncertainties may need to be considered when assessing the control scenario. Satellite data appear as a useful tool for the model evaluation and bridging some gaps in the absence of available observational data. The design of future studies should take these limitations into consideration.

Acknowledgements

This study was sponsored by U.S. EPA/Office of Air Quality Planning & Standards via contract #4-321-0210288 at North Carolina State University and by MEP at Tsinghua University, China. Thanks are due to the U.S. EPA for its technical support in CMAQ modeling.

References

Boylan, J. VISTAS, 2005. PM Model Performance Goal and Criteria. Presented at the National Regional Planning Organizations Modeling Meeting, Denver, CO, 2005.

Chameides, W.L., Luo, C., Salor, R., et al., 2002. Correlation between model-calculated anthropogenic aerosols and satellite-derived cloud optical depths: indication of indirect effect. Journal of Geophysical Research 107 (D10). doi:10.1029/2000JD000208.

Chen, B.Q., Yang, Y.M., 2005. Validation of MODIS aerosol optical thickness in the Taiwan Strait and its circumjacent sea area. Acta Oceanologica Sinica 27, 170–176.

Duan, F., He, K., Ma, Y., et al., 2006. Concentration level and chemical characteristic of atmospheric aerosol in Beijing: 2001–2002. Science Total Environment 335 (1–3), 264–275.

Fu, J.S., Streets, D.G., Jang, C.J., et al., 2009. Modeling regional/urban ozone and particulate matter in Beijing, China. Journal of Air and Waste Management Association 59, 37–44.

Geng, F., Tie, X., Xu, J., et al., 2008. Characterizations of ozone, NO_x, and VOCs measured in Shanghai, China. Atmospheric Environment 42 (29), 6873–6883.

He, K., Yang, F., Ma, Y., et al., 2001. The characteristics of $PM_{2.5}$ in Beijing, China. Atmospheric Environment 35 (29), 4959–4970.

Kim, S., Yoon, S., Kim, J., et al., 2007. Seasonal and monthly variations of columnar aerosol optical properties over east Asia determined from multi-year MODIS, LIDAR, and AERONET Sun/sky radiometer measurements. Atmospheric Environment 41 (8), 1634–1651.

Kumara, N., Chu, A., Foster, A., 2007. An empirical relationship between $PM_{2.5}$ and aerosol optical depth in Delhi Metropolitan. Atmospheric Environment 41 (21), 4492–4503.

Li, C.C., Mao, J., Lau, A.K.H., et al., 2003. Characteristics of distribution and seasonal variation of aerosol optical depth in eastern China with MODIS products. Chinese Science Bulletin 48 (22), 2488–2495.

Li, C.C., Mao, J.T., Lau, A.K.H., et al., 2005. Application of MODIS satellite products to the air pollution research in Beijing. Science in China Series D: Earth Sciences 48 (S2), 209–219.

Mi, W., Li, Z., Xia, X., et al., 2007. Evaluation of the moderate resolution imaging spectroradiometer aerosol products at two aerosol robotic network stations in China. Journal of Geophysical Research 112, D22S08. doi:10.1029/2007JD008474.

Morris, R., Koo, B., McNally, D., et al., 2005. Application of Multiple Models to Simulation Fine Particulate in the Southeastern U.S. Presented at the National Regional Planning Organizations Modeling Meeting, Denver, CO, 2005.

Paciorek, C.J., Liu, Y., Moreno-Macias, H., et al., 2008. Spatio-temporal associations between GOES aerosol optical depth retrievals and ground-level $PM_{2.5}$. Environmental Science and Technology 42 (15), 5800–5806.

Papayannis, A., Zhang, H.Q., Amiridis, V., et al., 2006. Extraordinary dust event over Beijing, China, during April 2006: Lidar, Sun photometric, satellite observations and model validation. Geophysical Research Letters 34, L07806. doi:10.1029/2006GL029125.

Pitchford, M.L., Malm, W.C., 1994. Development and applications of a standard visual index. Atmospheric Environment 28 (5), 1049–1054.

Streets, D.G., Fu, J.S., Jang, C.J., et al., 2007. Air quality during the 2008 Beijing Olympic games. Atmospheric Environment 41 (3), 480–492.

U.S. EPA (U.S. Environmental Protection Agency), 2007. Guidance on the Use of Models and Other Analyses for Demonstrating Attainment of Air Quality Goals for Ozone, $PM_{2.5}$, and Regional Haze. Office of Air and Radiation/Office of Air Quality Planning and Standards, U.S. EPA, Research Triangle Park, NC.

Wang, Q., Han, Z., Wang, T., et al., 2008. Impacts of biogenic emissions of VOC and NO_x on tropospheric ozone during summertime in eastern China. Science of the Total Environment 395 (1), 41–49.

Wang, J., Christopher, S.A., 2003. Intercomparison between satellite-derived aerosol optical thickness and $PM_{2.5}$ mass: implications for air quality. Geophysical Research Letters 30 (21), 2095. doi:10.1029/2003GL018174.

Wang, L., Xin, J., Wang, Y., et al., 2007. Evaluation of the MODIS aerosol optical depth retrieval over different ecosystems in China during EAST-AIRE. Atmospheric Environment 41 (33), 7138–7149.

Xu, J., Zhang, Y., Fu, J.S., et al., 2008. Process analysis of typical summertime ozone episodes over the Beijing area. Science of the Total Environment 399 (1–3), 147–157.

Zhang, Y., Vijayaraghavan, K., Wen, X.-Y., Snell, H.E., Jacobson, M.Z., 2009. Probing into regional O_3 and PM pollution in the U.S., part I. A 1-year CMAQ simulation and evaluation using surface and satellite data. Journal of Geophysical Research 114, D22304. doi:10.1029/2009JD011898.